Cognitive deficits and brain myo-Inositol are early biomarkers of epileptogenesis in a rat model of epilepsy

Rosaria Pascente a, Federica Frigerio a,Massimo Rizzi a, Luca Porcu b, Marina Boido c, Joe Davids d, Malik Zaben d, Daniele Tolomeo a, Marta Filibiana,1, WilliamP. Gray d, Annamaria Vezzani a, Teresa Ravizza

a Department of Neuroscience, IRCCS-Istituto di Ricerche Farmacologiche "Mario Negri", Milano, Italy
b Department of Oncology, IRCCS-Istituto di Ricerche Farmacologiche "Mario Negri", Milano, Italy
c Neuroscience Institute "Cavalieri Ottolenghi", Department of Neuroscience, University of Torino, Torino, Italy
d Neuroscience and Mental Health Research Institute, School of Medicine, Cardiff University, Cardiff, UK

Ab s t r a c t

One major unmet clinical need in epilepsy is the identification of therapies to prevent or arrest epilepsy development in patients exposed to a potential epileptogenic insult. The development of such treatments has been hampered by the lack of non-invasive biomarkers that could be used to identify the patients at-risk, thereby allowing to design affordable clinical studies. Our goal was to test the predictive value of cognitive deficits and brain astrocyte activation for the development of epilepsy following a potential epileptogenic injury. We used a model of epilepsy induced by pilocarpine-evoked status epilepticus (SE) in 21-day old rats where 60–70% of animals develop spontaneous seizures after around 70 days, although SE is similar in all rats. Learning was evaluated in the Morris water-maze at days 15 and 65 post-SE, each time followed by proton magnetic resonance spectroscopy

For measuring hippo campalmyo-Inositol levels, a marker of astrocyte activation. Rats were video-EEG monitored for two weeks at seven months post-SE to detect spontaneous seizures, then brain histology was done. Behavioral and imaging data were retrospectively analysed in epileptic rats and compared with non-epileptic and control animals. Rats displayed spatial learning deficits within three weeks from SE. However, only epilepsy-prone rats showed accelerated forgetting and reduced learning rate compared to both rats not developing epilepsy and controls. These deficits were associated with reduced hippocampal neurogenesis. myo-Inositol levels increased transiently in the hippocampus of SE-rats not developing epilepsy while this increase persisted until spontaneous seizures onset in epilepsy-prone rats, being associated with a local increase in S100β-positive astrocytes. Neuronal cell loss was similar in all SE-rats. Our data show that behavioral deficits, together with a non-invasive marker of astrocyte activation, predict which rats develop epilepsy after an acute injury. These measures have potential clinical relevance for identifying individuals at-risk for developing epilepsy following exposure to epileptogenic insults, and consequently, for designing adequately powered antiepileptogenesis trials.

Introduction

Epileptogenesis is a dynamic process of molecular, cellular and functional reorganization occurring in brain following precipitating events that lead to epilepsy (Pitkanen and Engel, 2014). Epilepsy is one of the most prevalent brain disorders affecting around 60 million people worldwide (Duncan et al., 2006). It is characterized by an enduring predisposition to generate spontaneous seizures often associated with cognitive and psychiatric comorbidities with negative social consequences. One major clinical need in epilepsy is to identify antiepileptogenesis treatments for preventing or arresting the development of the disease in patients who have been exposed to potentially epileptogenic brain insults, including status epilepticus (SE) (Holtkamp et al., 2005; Wagenman et al., 2014). The development of such treatments has been hampered by the lack of non-invasive biomarkers that could be used to identify the patients at-risk, thereby allowing to design affordable clinical studies (Engel et al., 2013; Pitkanen and Engel, 2014).

Our main goal was to test if cognitive deficits and astrocyte activation in seizure susceptible brain areas, both phenomena occurring in human epilepsy (Elger et al., 2004; Vezzani et al., 2012) and related animal models (Kleen et al., 2012; Vezzani et al., 2011), are biomarkers of epileptogenesis, thus predicting who is going to develop epilepsy after an acute brain injury. We used a well-established pilocarpine model of SE in 21 day-old rats where only a cohort of animals develops epilepsy (Marcon et al., 2009; Roch et al., 2002). This model mimics de novo SE in humans; SE is a relatively common clinical condition (10–41/ 100,000 population) (Betjemann and Lowenstein, 2015) with the majority of cases (54%) occurring in the absence of an antecedent diagnosis of epilepsy (Hesdorffer et al., 1998). 53% of patients (9/17)with de novo refractory SEwere reported to develop epilepsy (Holtkamp et al., 2005)
and in children with non-febrile convulsive SE subsequent epilepsy occurred in 13–74% of cases (Raspall-Chaure et al., 2006).

By focusing our analyses in the hippocampus, a key epileptogenic area in our animal model, we measured increased myo-Inositol (mIns) levels, a metabolite reflecting astrocyte activation (Brand et al., 1993) by in vivo proton magnetic resonance spectroscopy (1H-MRS) and cognitive deficits in the Morris Water Maze (MWM), a virtual version of which was recently developed in humans (Barkas et al., 2012). We found that both phenomena arise in rats before the onset of epilepsy, and predict which animals will develop the disease with high fidelity. Our results provide a proof-of-principle evidence of the potential predictive value of cognitive functions and mIns levels in seizure-prone brain areas for epilepsy development in individuals at high-risk following potential epileptogenic injuries.

Material and methods

2. Animals

2.1. Male Sprague–Dawley rats (Charles River, Calco, Italy) at postnatal day (PN) 21 (with PN1 defined as the day of birth) were used. The pups were housed with their dams at constant temperature (23 °C) and relative humidity (60%) with a fixed 12 h light–dark cycle and free access to food and water until weaning at PN21. Older animals were housed one per cage. For each experimental protocol described in Fig. 1, male pups were used from four independent litters. All experimental procedures were conducted in conformity with institutional guidelines that are in compliance with national (D.L. n.26, G.U. March

4, 2014) and international guidelines and laws (EEC Council Directive 86/609, OJ L 358, 1, December 12, 1987, Guide for the Care and Use of Laboratory Animals, U.S. National Research Council, 1996), and were reviewed and approved by the intramural ethical committee.

2.2. Induction and analysis of status epilepticus (SE) Lithium chloride (3 meq/kg; Merck Sharp & Dohme, Rome, Italy) was intraperitoneally injected in PN20 rats, 18 h before the subcutaneous injection of pilocarpine (Marcon et al., 2009; Roch et al., 2002) (60 mg/kg; Sigma-Aldrich, St. Louis, MO, USA). Controls were agematched rats injected with lithium chloride and an equivalent volume of vehicle (phosphate-buffered saline, PBS, pH 7.4) instead of pilocarpine. All animals received an injection of 10% sucrose in PBS, 2 h after the onset of SE to improve hydration. SE was not interrupted by any drug administration.

As in both adult and pediatric populations (DeLorenzo et al., 1995; Logroscino et al., 1997; Raspall-Chaure et al., 2006), the mortality rate in this SE model is relatively high. A total of 59 rats were injected with pilocarpine, and 23 rats died within the first week after SE. One rat was excluded from the study since he died during electrode implantation. The remaining 35 rats were used in two different protocols that were run sequentially (Protocol 2, n = 14 followed by Protocol 3, n = 21; Fig. 1). Since these animals were used for longitudinal 1H-MRS analysis, they could not be implanted with electrodes, therefore, SE was behaviourally scored by two independent investigators who observed rats for 6 h after pilocarpine injection. The following scores were used to monitor rats: score 1 (general automatisms and exploratory behavior) and score 2 (stage 5 seizures, bilateral forelimb clonus with rearing and falling). For each score, we determined the time of appearance of the first sign. Retrospective score analysis was done after rats were identified as epileptic or non-epileptic (see later): Score 1 (min), non-epileptic 5.0±1.0, n=20; epileptic, 4.5±0.7, n=11; Score2 (min), none pileptic 12.1 ± 0.6; epileptic, 10.4 ± 0.6. The onset of SE was determined by the time of appearance of the second stage 5 seizure and was similar in non-epileptic (13.5 ± 0.6, n = 20) and epileptic rats (13.2 ± 0.7, n=11): after this time stage 5 seizures similarly recurred in both groups for the 6 h observation period. The two investigators confirmed concordance of these measures in each animal at completion of the observation period.

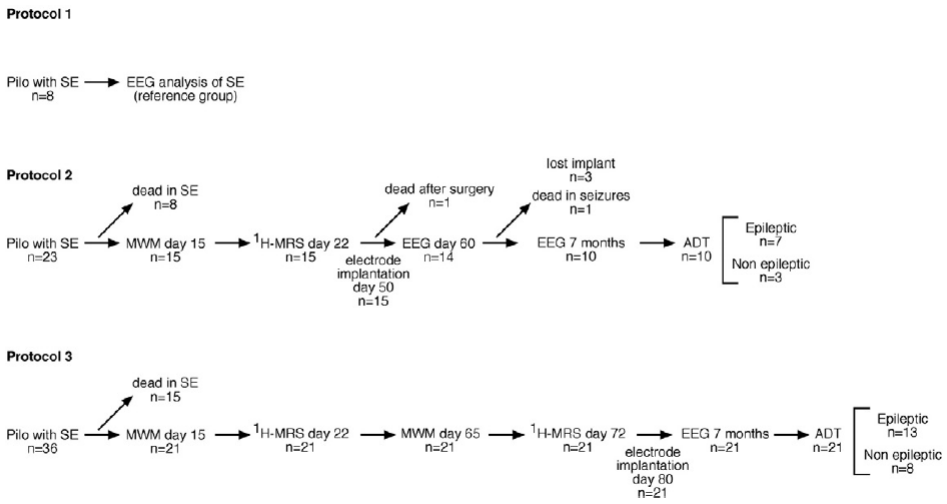

Fig. 1. The schematic diagram illustrates the experimental design, the number of rats injected with pilocarpine (Pilo with SE) and undergoing the subsequent analyses, and the animals excluded by the study in each experiment. Protocol 1 refers to rats exposed to SE

and used as a reference group to determine by EEG analysis that SE severity and duration were similar in all animals. Protocol 2 refers to rats tested in the MWM at day 15 post-SE then subjected to 1H-MRS analysis (day 22) and electrode implanted at day 50 for EEG analysis to detect epilepsy onset. After electrode implantation these rats did not undergo additional behavioral or 1H-MRS analyses until seizure detection was done at 7 months (as in Protocol 3). Protocol 3 refers to rats followed for 7months and longitudinally tested for cognitive behavior in theMWMat day 15 and day 65 post-SE, each time followed after seven days by 1H-MRS analysis ofmIns. After imaging sessionswere terminated, rats were electrode implanted at day 80 post-SE for seizure detection at 7months. All rats were tested for afterdischarge threshold (ADT) at the end of EEG recordings. Brain histology was done after animals were sacrificed at the end of the experiment.

We used an additional cohort of rats (n=8) implanted with hippocampal electrodes at PN19 and injected with lithium and pilocarpine at PN20 and PN21, respectively, to determine by EEG analysis if SE was of similar severity and duration in all animals (Protocol 1, Fig. 1). SE onset was defined by the appearance of continuous spikes with amplitude N2- fold baseline and frequency N 5Hz while the end of SE was set as the time the inter-spike interval becomes consistently N2 s (Pitkanen et al., 2005). Spikes were defined as sharp waves with an amplitude at least 2-fold higher than the baseline and a duration of N20 ms, or as a spike-and-wave with a duration of b200 ms (Pitkanen et al., 2005). Electrode-implanted rats were continuously (24/7) EEG recorded from 30 min before pilocarpine administration (to assess EEG baseline activity) until 48 h after injection. The EEG analysis showed that the onset of SE (16.0 ± 1.1 min), its duration (22.6 ± 0.5 h), the temporal distribution of spikes (Clampfit v10.0; Axon Instruments, Union City, CA, U.S.A), and the power spectral densities distribution of 5 frequency bands (delta: 1–4 Hz; theta: 4–8 Hz; alpha: 8–13 Hz; beta: 13–30 Hz; gamma: 30–40 Hz; Lab Chart, AD Instrument Ltd., Oxford, UK) during the first 3 h of SE were similar in all animals (not shown). After SE monitoring, these rats were not further investigated since they were only used as a "reference" group for rats where SE was behaviorally scored (see above).

2.3. Detection of recurrent spontaneous seizures and after discharge threshold Rats undergoing EEG recordings (Fig. 1) were electrode implanted under general gas anesthesia (1.4% isoflurane in a mixture of 70% N2O-30%O2). A bipolar nickel-chrome wire-insulated electrode (60 µm) was implanted unilaterally randomly in the septal left or right pole of the hippocampus at the following coordinates from bregma: mm: anteroposterior [AP] −3.3; nose bar −2.5 mm, L ± 2.4 and 3 mm below dura mater (Paxinos and Watson, 2005). Moreover, a cortical electrode was implanted onto the somatosensory cortex in the contralateral hemisphere. The electrodes were connected to a multipin socket and secured to the skull by acrylic dental cement.

In this SE model, spontaneous seizures typically develop after a latent phase of around 70 days (Dubé et al., 2001; Leroy et al., 2011). To double check the duration of the latent phase in our experimental conditions, the 14 rats of Protocol 2 were video-EEG recorded (24/7) from day 60 to day 75 post-SE (Fig. 1). According to the literature evidence, spontaneous seizures were detected at day 68.8 ± 1.8 (2.8 ± 0.6 seizures in 2 weeks) in 5 rats, denoting that this was the time approaching epilepsy onset. After day 75, 3 rats still without seizures lost their EEG implant and one rat died during severe seizures, therefore these animals were excluded from this study. The 10 remaining rats were again video- EEG recorded at 7 months post-SE: 7 rats

developed spontaneous seizures (epileptic; which includes the 5 rats already developing epilepsy around day 70) while 3 rats did not develop seizures (non-epileptic). Since data showed that the latent phase in this model lasts for at least 70 days, we carried out our longitudinal behavioral and MRI analyses within this time frame.

Rats in Protocol 3 (n = 21; Fig. 1) were video-EEG monitored at 7 months post-SE for two weeks (24/7) to determine and quantify spontaneous seizures. We found that 13 out of 21 rats developed spontaneous motor seizures (epileptic) while the remaining 8 rats showed no seizures (non-epileptic). Therefore the average incidence of epilepsy in this model (5.8 ± 1.5 seizures in 2 weeks in Protocols 2 and 3) was between62% and 70%, in agreement with previous studies where animals were recorded at least 3 months post-SE (Kubova et al., 2004; Marcon et al., 2009).

We also measured the rat hippocampal after discharge threshold (ADT) at the end of EEG monitoring as a measure of local excitability. Animals were electrically stimulated via the hippocampal electrode, using constant current stimulus (1 ms monopolar square waves, 50 Hz for 2 s). Determination of the ADT was done using an ascending stepwise procedure (Frigerio et al., 2012). The initial stimulus intensity was 50 µA and was increased by 10 µA up to 100µA, and then by 100 µA up to a maximal value of 400 µA by intervals of 1min, until one AD of at least 10 s duration was elicited. ADT was reduced by 50% in epileptic rats (103 ± 18 µA; n = 20) compared to control rats not exposed to SE (220± 40 µA, n=9). Non-epileptic rats showed an ADT similar to control rats (223 ± 22 µA, n=11). AD duration did not differ among the 3 experimental groups (sec; control: 19.1±2.6; non-epileptic: 23.3±4.0; epileptic: 26.0±6.1). Twenty-four hours later, rats were killed for brain histological analysis.

2.4. Morris water maze (MWM) The MWM apparatus consisted of a circular pool (diameter 150 cm, height 60 cm) filled with water, opaque by the addition of a brown food dye (depth 30 cm, temperature 25±1 °C). The circular pool was ideally divided in four quadrants, and a squared platform (11 × 11 cm) was placed 1 cm below the water surface in the center of one quadrants. The test was performed twice in the same rat, at day 15 and day 65 post-SE, unless otherwise indicated (Fig. 1). The position of the platform was kept in the same quadrant during the first behavioral test, then was moved to a different quadrant during the second exposure to the same behavioral test. Each rat underwent one training session per day, which included four swims; daily training sessions were done for five consecutive days. During each training session, rats were placed into the pool starting from each of the four quadrants (north, west, south and east) with the head facing towards the wall of the pool. The escape latency, i.e. the time to reach the hidden platform, was measured. Each rat was allowed to swim until the platform was found or rat had swum unsuccessfully for 60 s. In the latter case, the rat was guided to the platform by the investigator and its escape latency was recorded as 60 s. After 10 s rest on the platform, the rat was transferred into its home cage.

Rat movements were monitored by a video camera connected to a digital tracking device (Noldus, Ethovision, The Netherlands). 2.5. 1H-MRS analysis and spectra quantification Animals were imaged at day 22 and day 72 post-SE, i.e., seven days after the MWM test (Fig. 1), under general gas anesthesia (1.4% isoflurane in a mixture of 70% N2O-30%O2). Respiratory rate and temperature were continuously monitored. Experiments were done on a 7T Bruker Biospin 70/30 Avance III system, equipped with a 12 cm diameter gradient coil

(400 mT/m maximum amplitude). A transmit cylindrical radio frequency (rf) coil (7.2 cm inner diameter) and a receive surface rf (2 × 2 cm) coil array positioned over the animal head were used. Localized proton spectroscopy was performed as previously described (Filibian et al., 2012). Briefly, a PRESS (Point Resolved Spectroscopy) sequence (repetition time TR/TE = 2500/10 ms, 512 scans, spectral width 20 ppm, 8192 points) was carried out in a single voxel (14 µL) positioned randomly in the septal left or right pole of the hippocampus. Water suppression was performed with VAPOR and first and second order shims were adjusted using FASTMAP (Fast, Automatic Shimming technique by Mapping Along Projections). 1H-MRS spectra were quantified using TARQUIN 4.2.1 (Wilson et al., 2011) for the estimation of mIns levels. Each spectrum was pre-processed by applying automated zero-order phasing and referencing, and by performing residual water line removal with the HSVD method. The processed signal was fit to a linear combination of selected metabolites. The reliability and quality of the fitting procedure was assessed both by visual inspection and by checking the quality parameter Q retrieved by TARQUIN The mean value of Q was included between 1.15 and 1.3, indicating a very high fit quality (Q= 1 corresponds to a perfect fit) (Wilson et al., 2011). The amplitudes of the mIns signals obtained by the fit that had a CRLB (Cramer-Rao lower bound) higher than 35% were excluded from the results. Relative mIns levels were then derived by scaling the fitted amplitudes by the amplitude of the total Creatine (tCr: Cr + phospho Cr) signal, considered as the internal standard.

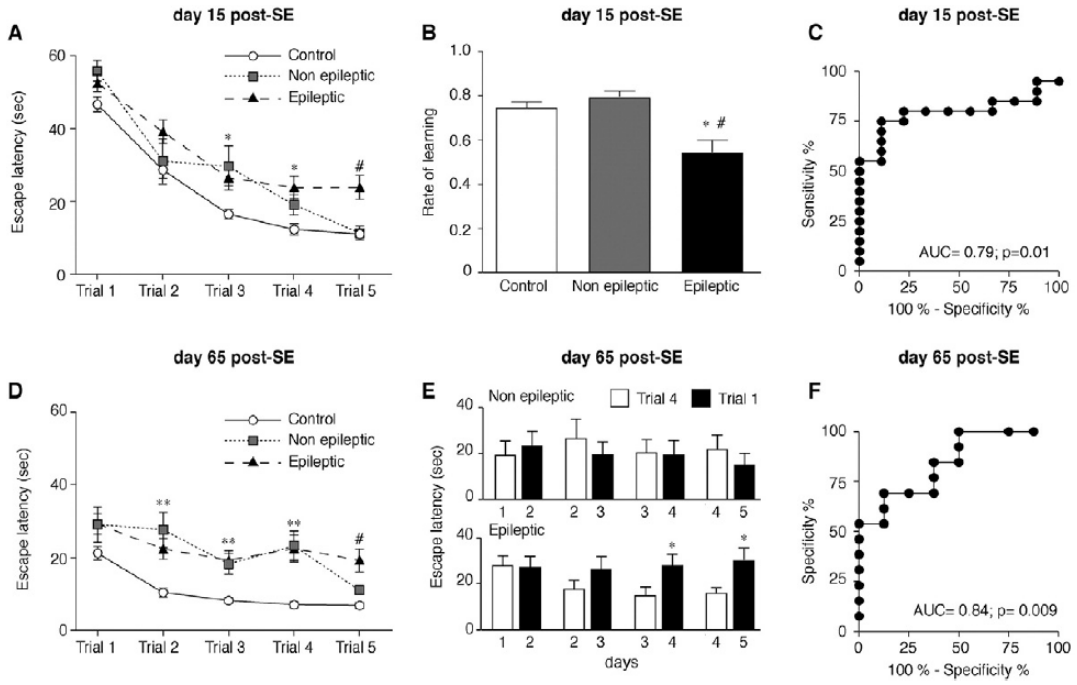

Fig. 2. Cognitive performance in Morris Water Maze during epileptogenesis. Panel A depicts the escape latency during the 5 days of training in controls (n=33), non-epileptic (n=11) and epileptic rats (n=20) at day 15 post-SE. *p b 0.05 vs control; #pb 0.05 vs non-epileptic, by one-way ANOVA followed by Dunn's test. Panel B shows the rate of learning at 15 days after SE: the difference between the escape latency in trials 1 and 5, normalized to the escape latency in trial 1. Epileptic rats showed a slower rate of learning compared to non-epileptic rats and controls *p b 0.05 vs control; #pb 0.05 vs non-epileptic by one-way ANOVA followed by Dunn's test. Panel C depicts the ROC curve obtained by comparing the rate of learning of epileptic vs

non-epileptic rats; the AUC = 0.79 indicates that this parameter discriminates with good accuracy the two cohorts of animals. Panel D depicts the escape latency during the 5 days of training in controls (n = 32), non-epileptic (n = 8) and epileptic rats (n = 13) at day 65 post-SE. **p b 0.01 vs control; #p b 0.05 vs non-epileptic, by one-way ANOVA followed by Dunn's test. Panel E shows daily comparison during the 5 days of training of the escape latency measured during the last training session of each day (Trial 4) with the escape latency measured during the first session of the subsequent day (Trial 1) at 65 days post-SE in epileptic and non-epileptic rats. Epileptic rats had poorer overnight retention (i.e. accelerated forgetting) compared to non-epileptic rats. *p b 0.05 vs trial 4 at days 3 and 4. Panel F depicts the ROC curve obtained by comparing the accelerated forgetting of epileptic vs nonepileptic rats; the AUC = 0.84 indicates that this parameter discriminates with excellent accuracy the two cohorts of rats.

2.6. Tissue preparation for immunohisto chemical analysis

Twenty-four hours after measuring the ADT, rats were deeply anaesthetized using ketamine (150 mg/kg) and medetomidine (2.0 mg/kg) and perfused via ascending aorta as previously described (Marcon et al., 2009). The brains were post-fixed for 90 min at 4 °C, transferred to 20% sucrose in PBS for 24 h at 4 °C, frozen in n-pentane for 3 min at −50 °C, and then stored at−80 °C until assayed. Immunohistochemistry (IHC) was done to detect glia activation (S100β for astrocytes; OX- 42 for microglia) and neurogenesis (double cortin, DCX). Nissl staining was performed to assess neuronal cell loss. All the analyses were done in 6 vehicle-injected rats (controls) and 14 pilocarpine-treated rats (n=7 epileptic;n=7non-epileptic) randomly taken among the rats included in Protocols 2 and 3 (Fig. 1), except for stereological counting and neurogenesis that was done in 5 randomly chosen rats in each group. Serial coronal sections (40 µm) were cut on a cryostat throughout the septo-temporal extension of the hippocampus (−2.3 to −5.8 mm from bregma) according to Paxinos & Watson atlas (Paxinos and Watson, 2005). We prepared 8 series of 10 sections each (4 series including the septal and 4 series including the temporal aspect of the hippocampus). In each series, the 1st and 5th sections were stained for Nissl. In the 1st, 3th, 6th and 8th series, the 2th section was stained for S100β, the 3rd for OX-42 and the 4th for DCX. S100β, OX-42 and DCX immunostaining was carried out as previously described (Filibian et al., 2012; Iori et al., 2013). We previously established lack of signal when slices were incubated with the primary antibodies pre absorbed with the corresponding peptides, or without the primary antibodies. Immunohistochemical analysis of brain sections (plates 19–22) (Paxinos and Watson, 2005) and quantification procedures were performed by two independent expert investigators blind to the identity of the samples.

Neuronal cell loss was quantified by reckoning the number of Nisslstained neurons in CA1 and CA3 pyramidal cell layers and the hilar interneurons using an image of the whole hippocampus captured at 20× magnification (Virtual Slider Microscope; Olympus, Germany) and digitized (n = 6 control; n = 7 epileptic; n = 7 non-epileptic; 4 slices/rat). In addition, stereological analysis in Nissl-stained sections was performed (n=5 each group; 3 slices/rat). The nucleoli of pyramidal neurons (CA1 and CA3) and hilar interneurons were counted at 40× magnification using an Eclipse E600 microscope equipped with Optronics Micro Fire digital camera (Nikon, Japan). The neuronal density was estimated with the Optical Fractionator technique, using a computer-assisted microscope and the Stereo Investigator software (Micro Bright Field), as previously described (Spigolon et al., 2010). A 4 µm guard zone, a 50 µm × 50

µm counting frame size and a 100 µm × 100 µm grid layout were employed. Data obtained in both hippocampi in each rat were averaged, thus providing a single value for each rat, and this value was used for the statistical analysis.

The total number of S100β-immunore active astrocytes was counted in the whole hippocampus (20× magnification) by an investigator who visually identified the cells; then an automated cell count was generated using ImageJ software (n=6 control;n=7epileptic;n=7nonepileptic; 2 slices/rat).

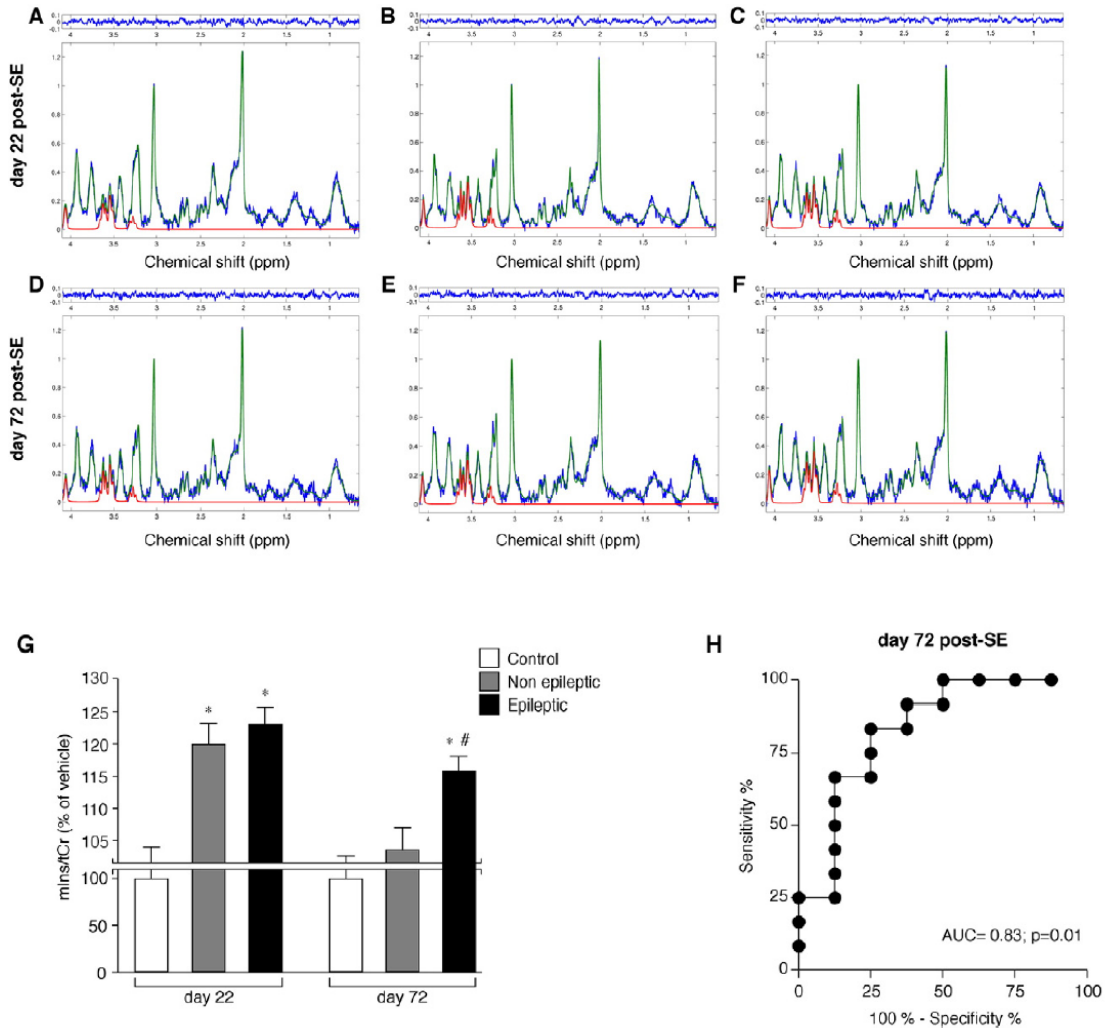

Fig. 3. 1H-MRS analysis of mIns/tCr levels in the hippocampus during epileptogenesis. Representative 1H-MRS spectra acquired at day 22 (A-C) or day 72 (D-F) post-SE in control (A,D), nonepileptic (B,E) and epileptic rats (C,F). Spectra and fit residuals (upper row) are plotted in blue, metabolite fits are plotted in green, and mIns contribution is plotted in red. Panel G depicts the mIns/tCr levels (mean ± s.e.m.) in the various experimental groups at day 22 (controln = 9; non-epileptic n=11; epileptic n=20) and day 72 (control n = 9; non epilepticn = 8; epileptic n=13) post-SE. At day 22,mIns/tCr levelswere increased similarly in epileptic and non-epileptic rats compared to controls while at day 72 themIns/tCr increase persisted only in epileptic rats. *p b 0.05 vs control; #pb 0.05 vs non-epileptic by one-way ANOVA followed by Dunn's test. Panel H depicts the ROC curve obtained by comparing

mIns/tCr levels in epileptic vs non-epileptic rats at day 72 post-SE; the AUC = 0.83 indicates that this parameter discriminate with excellent accuracy the two cohort of rats.

OX-42-immunostained area was measured in the whole hippocampus (20× magnification) using ImageJ software, and data were expressed as positive pixels/total assessed pixels; the percent area with the specific staining was used for subsequent statistical analysis (n= 6 control; n=7epileptic; n = 7 non-epileptic; 2 slices/rat). The analysis of DCX-immunostained sections (n=5 rats each group; 4 slices/rat)was performed using a Zeiss slide scanner (Axioscanner Z1, Zeiss, Germany) and a Zeiss ZEN2 software (v1.0 EN 1.0) at 5×, 10× and 20× magnifications, and each hippocampus was reconstructed into a tiled image using Zeiss software. DCX-positive cells in the subgranular zone were counted in each dentate, as previously described (Zaben et al., 2009). For Sholl analysis, one DCX-stained cell/dentate blade/dentate/ section was randomly chosen and the dendritic tree was analysed using ImageJ software (FIJI, v2.0.0-rc-43/150e) with the Simple Neurite Tracer Plug-in. Sholl analysis was confined to DCX-positive cells with a dendritic tree extending into the molecular layer. Dendritic processes were semi-automatically traced in ImageJ (v1.49, NIH), and the number of dendritic intersections across concentric Sholl circle radii rings at intervals of 10 µm was recorded.

2.7. Randomization, blinding procedures and statistical analysis of data Sample size was a priori determined based on previous experience with the animalmodel and the respective behavioral and imaging analyses. Simple randomization was applied to assign a subject to a specific experimental group (vehicle or pilocarpine treatment) using a web site randomization program (http://www.randomization.com). One day after vehicle or pilocarpine injection, rats were linked to numerical identifiers by an external investigator not involved in the study and unaware of the treatment. This procedure ensured that animal handling and data acquisition during the longitudinal analyses were done by investigators blinded to the identity of the animals. After epileptic and non-epileptic rats were identified based on the presence of spontaneous seizures at 7 months, the external investigator generated two considered excellent for AUC values close to 1. Differenceswere considered significant with a p b 0.05.

3. Results

After grouping the animals at 7months post-SE in epileptic and nonepileptic rats, based on the presence of spontaneous seizures and the ADT, we retrospectively analysed and compared their behavioral performance in the MWM (Fig. 2) and their respective mIns levels by 1HMRS (Fig. 3) that were both assessed before the predicted time of epilepsy onset.

3.1. Evaluation of animal performance in Morris Water Maze During the 5 days of training, the overall statistical analysis indicates that the three experimental groups (control, non-epileptic and epileptic rats) performed differently both at day 15 (Fig. 2A) and at day 65 (Fig. 2D) post-SE [Group x Trial interaction: day 15: $F(8,236) = 1.95$, p b 0.05; day 65: $F(8,200) = 1.98$, p b 0.05]. At day 15, all rats learned to find the hidden platform independently of the experimental group, as indicated by the progressive reduction in the escape latency over the 5 training days (Fig. 2A). However, epileptic and non-epileptic rats had a 2-fold longer escape latency on average than controls in trials 3 and 4 (Fig. 2A; p b 0.05). In trial 5, this deficit was maintained only in epileptic rats (Fig. 2A; p b 0.05). In accordance, the escape latency did not improve during the last 3 trials in epileptic rats (p b 0.05 vs both control and non-epileptic

rats). Epileptic rats also showed a slower rate of learning (p b 0.05) compared to non-epileptic rats and controls (Fig. 2B). The ROC curve obtained by comparing the rate of learning of epileptic vs none pileptic rats showed an AUC=0.79 (p=0.01; Fig. 2C). At day 65 post- SE, the learning performance of the three experimental groups was similar to day 15 (Fig. 2D vs A). Notably, a new behavioral feature was specifically observed in epileptic rats: comparison of the escape latency of the last training session of each day with the escape latency of the first training session of the subsequent day showed that epileptic rats had a poor overnight memory retention (i.e., accelerated forgetting) compared to non-epileptic rats, a phenomenon developing over the 5 day trials (Fig. 2E). The correspondent ROC curve had an AUC value of 0.84 (p=0.009; Fig. 2F). In SE-exposed rats, we did not observe any clinical seizure during the training period.

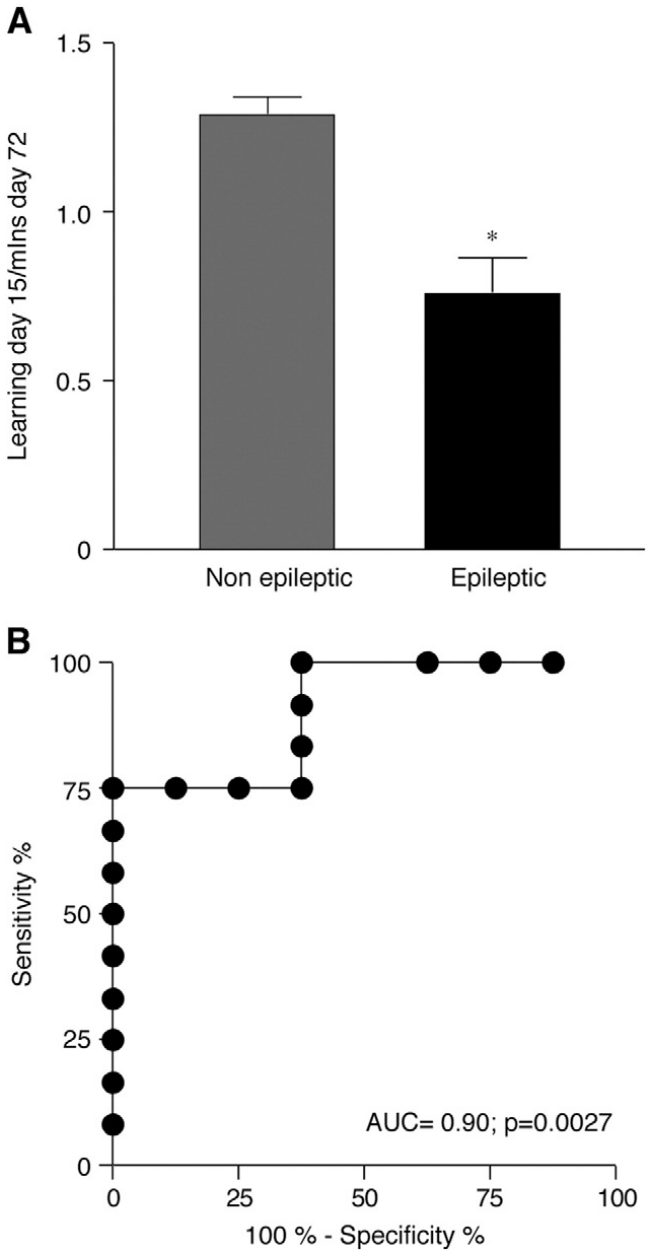

3.2. 1H-MRS analysis of mIns

One week after the end of each behavioral test, all rats underwent 1H-MRS analysis in the dorsal hippocampus for measuring mIns levels (Fig. 3). At day 22, mIns/tCr levels increased by 20% on average in both epileptic and non-epileptic rats compared to controls (0.59 ± 0.02 arbitrary unit; Fig. 3A–C, G). At day 72, this increase persisted only in epileptic rats (Fig. 3F,G)whilemIns/tCr levels declined in non-epileptic rats to control levels (Fig. 3E,G). The ROC curve comparing epileptic vs nonepileptic rats at day 72 showed an AUC = 0.83 (p= 0.01).

The accuracy of discrimination between SE-rats thatwill develop epilepsy from those rats not developing the disease was increased by reckoning the ratio between rate of learning at day 15 and mIns/tCr levels at day 72 (Fig. 4A) as shown by the ROC curve with an AUC = 0.9 (p = 0.0027; Fig. 4B).

3.3. Brain histology

At completion of EEG recording and ADT measurements, we analysed cell loss, glia activation and neurogenesis in the septal pole of the hippocampus of randomly selected rats since this area is especially involved in cognitive processes (Broadbent et al., 2004).

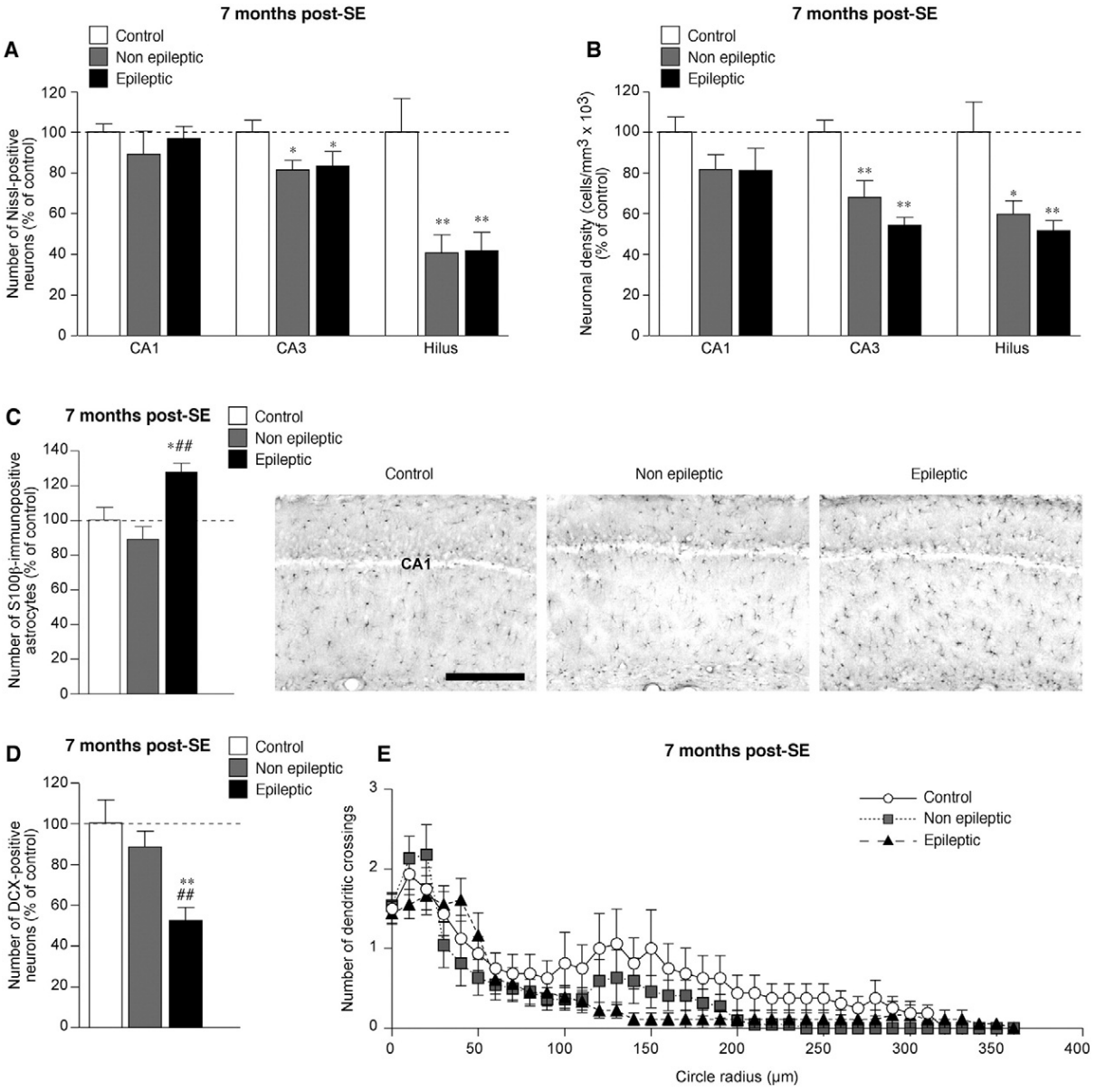

Fig. 5. Histological analysis of the hippocampus at 7 months post-SE in rats with and without spontaneous seizures. Panels A and B depict the quantification of neuronal cells in CA1 and CA3 pyramidal layers and in the hilus estimated by counting the Nissl-stained neurons (A) and by stereological analysis (B) in control (n=5–6), non-epileptic (n=5–7) and epileptic (n=5–7) rats. In control hippocampi, the number of neuron/section was (mean±s.e.m., n=6) CA1: 1279±25; CA3: 546±15; hilus: 93.9±7 (A); cells/mm3 x 103 (mean±s.e.m., n=5) CA1: 159.1 ± 12.1; CA3: 95.3 ± 5.8; hilus: 11.2 ± 1.8 (B). *p b 0.05, **p b 0.01 vs control by one-way ANOVA followed by Dunn's test. Panel C shows the number of S100β-immunoreactive astrocytes in control (n = 6), non-epileptic (n = 7) and epileptic (n = 7) rats. The number of cells (mean ± s.e.m., n = 6) in control was 1.891 ± 139. Microphotographs in panel C depict representative images of S100β-positive astrocytes in CA1 pyramidal cell layer in the various groups. *p b 0.05 vs control, ##p b 0.01 vs non-epileptic by one-way ANOVA followed by Dunn's test. Scale bar: 100 µm. Panel D depicts the quantification of DCX-positive neurons in the dentate gyrus in the various experimental groups (n= 5 rat each group). The number of DCX cells in control was 66.8 ± 8 (mean ± s.e.m.). **p b 0.01 vs control, ##p b 0.01 vs non-

epileptic by one-way ANOVA followed by Dunn's test. Panel E shows Sholl analysis in epileptic and non-epileptic rats showing similar compromission in dendrite complexity.

3.3.1. Neuronal cell loss

A reduction of the total number of hilar interneurons (by 60% on average; p b 0.01 vs control) and CA3 pyramidal cells (by 18% on average; p b 0.05 vs control, n = 6) was found in all SE-rats independently on whether or not they developed spontaneous seizures (Fig. 5A; n=7 epileptic, n = 7 non-epileptic). Stereological analysis confirmed that cell loss was similar in all rats showing around 55% reduction of hilar interneurons (p b 0.05) and 40% reduction of CA3 pyramidal cells (p b 0.01) vs controls (Fig. 5B) (n=5 each group). The number of CA1 pyramidal neurons was not significantly reduced in SE-rats compared to controls (Fig. 5A, B).

3.3.2. Glia activation

OX-42-positive microglia showed small cell bodies and extensive ramifications denoting their resting state in all three experimental groups (not shown). Accordingly, the percent hippocampal area occupied by the specific OX-42 signal in epileptic (10.6 ± 0.6%, n = 7) and non-epileptic (8.5 ± 1.1%, n = 7) rats was similar to control rats (9.4 ± 0.8%, n = 6).

Differently, we found that the number of S100β-positive astrocytes was increased by 27.1±5.2% in epileptic rats (n=7, p b 0.05) compared to controls (n=6) while no difference was found between non-epileptic (n= 7) and control rats (Fig. 5C).

3.3.3. Neurogenesis

There was an overall significant difference in the number of newly born DCX-positive neurons in the dentate gyrus among the three experimental groups (p b 0.01). A significant 50% reduction in these cells was found in epileptic vs control rats while non-epileptic rats were similar to controls (Fig. 5D; n=5 each group). The dendritic arborization of DCX positive cells with dendrites extending through the granule cell and molecular layers was examined in 18 cells from epileptic rats, 22 cells from non-epileptic rats and 16 cells from control rats using Sholl analysis. The analysis of the AUC of the mean crossings per cell showed a significant effect of the group (p b 0.01) revealing differences between epileptic and control rats (p b 0.01) and non-epileptic and control rats (p b 0.05) (Fig. 5E). Epileptic and non-epileptic rats had less complex dendritic trees, especially distally, with this phenomenon more marked, although not significantly, in epileptic rats (Fig. 5E).

4. Discussion

We report the novel evidence that cognitive deficits in a spatial memory test together with astrocyte activation in the hippocampus, predict the development of epilepsy in a rat model of de novo SE with high accuracy. This model is highly valuable for determining factors associated with epilep to genesis since only a cohort of rats develop spontaneous seizures after an inciting event of similar severity and duration (Marcon et al., 2009; Roch et al., 2002). In accord, we found that only 70% of rats developed epilepsy, although SE was similar in all rat. In support, hippocampal cell loss, an objective measure of SE severity (Fujikawa, 1996), did not differ among animals.

We identified epileptic and non-epileptic rats based on the detection of video-EEG seizures at 7 months post-SE. We monitored rats for two weeks, which allows seizure detection based

on their mean frequency, i.e., one seizure every three days. Although we cannot exclude that seizures might have occurred at later time points in non-epileptic rats, this is unlikely based on literature evidence related to this model (Kubova et al., 2004). Additionally, ADT in non-epileptic and control rats was similar while it was significantly reduced in epileptic rats, thus supporting the lack of chronic excitability changes in rats without seizures.

Our retrospective data analysis showed that SE-exposed rats developed early cognitive deficits in a spatial learning task. Impaired cognitive functions were previously reported to occur before epilepsy onset during both post-natal development (Cilio et al., 2003; Kubova et al., 2004; Liu et al., 1994; Sayin et al., 2004) and in adulthood (Chauviere et al., 2009; Hort et al., 2000; Jones et al., 2010) but it was unknown whether these deficits correlated with epilepsy development. We describe for the first time that a reduced rate of learning and an accelerated forgetting are two specific features of rats prone to develop epilepsy, and these deficits anticipate the onset of spontaneous seizures.

Notably, impaired spatial learning and accelerated forgetting were also described in temporal lobe epilepsy (TLE) patients exposed to a virtual MWM task (Barkas et al., 2012) and cognitive deficits were documented in children and adult before the first recognized seizures or at the early stages of the disease (Hermann et al., 2006; Oostrom et al., 2003; Witt and Helmstaedter, 2015). This clinical evidence highlights the high translational significance of our findings.

Our results, together with evidence that cognitive deficits and the propensity to develop epilepsy after SE both increase with age (Cilio et al., 2003; Kubova et al., 2004; Sayin et al., 2004), reinforce the hypothesis that they share common molecular changes (Devinsky et al., 2013; Todd et al., 2006). In this respect, we found that persistent astrocyte activation in the hippocampus is a specific feature of epilepsy-prone rats, as shown by longitudinal 1H-MRS analysis of mIns/tCr levels and by post-mortem analysis of S100β-positive astrocytes. Similar changes in these measures were reported in adult rat models where all animals develop epilepsy (Filibian et al., 2012; Wu et al., 2015; Zahr et al., 2009). Altogether, these data suggest that S100β-expressing astrocytes contribute to the mIns changes during epilepto genesis and may play a role in both cognitive impairment and seizure generation. Accordingly, mice overexpressing S100β show spatial memory impairment (Gerlai et al., 1995) while S100β knock-out mice exhibit enhanced spatial learning in the MWM (Nishiyama et al., 2002). S100β-induced modifications of intracellular Ca2+ in astrocytes (Barger and Van Eldik, 1992) and in neurons by activation of RAGE receptors (Huttunen et al., 2000) appear to be involved in the modulation of synaptic plasticity. S100β released by astrocytes may also promotes changes in neuronal rhythms that are relevant for seizure onset (Morquette et al., 2015; Sakatani et al., 2008), and RAGE receptors are implicated in both cognitive impairments (Mazarati et al., 2011) and epileptogenesis (Iori et al.,2013). In this context, there is increasing evidence that activated astrocytes play a key role in neuronal network hyperexcit ability underlying seizures (Devinsky et al., 2013; Robel et al., 2015).

Neurogenesis is another biological process implicated in cognitive dysfunctions in TLE (Hattiangady et al., 2004; Scharfman and Gray, 2007) and aberrant neuronal network excitability (Scharfman et al., 2000). In particular, a negative correlation was reported between the number of DCX-positive neurons in surgically resected TLE hippocampi and the

memory functions in the respective patients before surgery (Coras et al., 2010). Our data show that epileptic rats had reduced levels of dentate neurogenesis compared to controls and non-epileptic rats. Altered neurogenesis is present immediately after SE during epileptogenesis (Gray and Sundstrom, 1998; Parent et al., 1997), at the time of our behavioral analysis, as well as chronically in TLE (Hattiangady et al., 2004), and thus might contribute to the progressive cognitive impairment we observed in rats prone to develop epilepsy. Other cellular alterations induced by SE such as reduction in dendritic spine density (Jiang et al., 1998) and place cells dysfunctions (Holmes, 2015) have been associated with cognitive impairment (Holmes, 2015; Jiang et al., 1998) and could play a role, together with the less complex dendritic arborization of DCX-positive neurons in SE-rats, to the behavioral deficits that precede epilepsy development in our model.

5. Conclusions

This study provides the first proof-of-principle demonstration that assessment of cognitive abilities and 1H-MRS analysis of mIns in seizure-prone brain areas following potential epileptogenic injuries may represent clinically meaningful biomarkers for early identification of individuals at high-risk for developing epilepsy (Betjemann and Lowenstein, 2015; Herman, 2002; Raspall-Chaure et al., 2006). Although our findings are related to a model of SE-induced epilepsy, increased mIns brain levels were found to be associated with neurological dysfunctions in children and adults after traumatic brain injury (Ashwal et al., 2004; Brooks et al., 2000; Garnett et al., 2000), although no attempts were made to correlate these measures with epilepsy development. This evidence, therefore, potentially extends the significance of our findings to epileptogenic injuries other than SE, such as neurotrauma, ischemic stroke or CNS infections. If applied and validated in the clinical setting these non-invasive measures could greatly facilitate the clinical development of novel preventive antiepileptogenic therapies.

Author contributions

R. Pascente injected rats with pilocarpine and conducted the behavioural and immunohisto chemical experiments under the supervision of T. Ravizza; F. Frigerio implanted and monitored rats for seizure detection and measured ADT; M. Rizzi analysed EEG tracings; L. Porcu conducted statistical analysis of data; M. Boido performed stereological analysis; J. Davids and M. Zaben performed neurogenesis analysis with the supervision of W. P. Gray; D. Tolomeo and M. Filibian conducted 1H-MRS analysis and related spectra quantification; W. P. Gray participated to manuscript writing and editing; T. Ravizza and A. Vezzani supervised all phases of the project and wrote the manuscript. The authors thank Dr. F. Noè for his contribution in the preliminary phase of this study, and Mr. F. De Ceglie for his technical assistance in the preparation of figures.

Conflict of interest

The authors declare no competing financial interests.

Acknowledgements

This work was supported by the European Union Seventh Framework Programme (FP7/2007-2013) under grant agreement n. 602102 (EPITARGET; AV), Fondazione Monzino (5600) (AV), CURE (AV) and Epilepsy Research UK (F1204Zaben; WPG).

References

Ashwal, S., Holshouser, B., Tong, K., Serna, T., Osterdock, R., Gross, M., et al., 2004. Proton spectroscopy detected myoinositol in children with traumatic brain injury. Pediatr. Res. 56, 630–638.

Barger, S.W., Van Eldik, L.J., 1992. S100 beta stimulates calcium fluxes in glial and neuronal cells. J. Biol. Chem. 267, 9689–9694.

Barkas, L., Redhead, E., Taylor, M., Shtaya, A., Hamilton, D.A., Gray, W.P., 2012. Fluoxetine restores spatial learning but not accelerated forgetting in mesial temporal lobe epilepsy. Brain 135, 2358–2374.

Betjemann, J.P., Lowenstein, D.H., 2015. Status epilepticus in adults. Lancet Neurol. 14, 615–624.

Brand, A., Richter-Landsberg, C., Leibfritz, D., 1993. Multinuclear NMR studies on the energy metabolism of glial and neuronal cells. Dev. Neurosci. 15, 289–298.

Broadbent, N.J., Squire, L.R., Clark, R.E., 2004. Spatial memory, recognition memory, and the hippocampus. Proc. Natl. Acad. Sci. U. S. A. 101, 14515–14520.

Brooks, W.M., Stidley, C.A., Petropoulos, H., Jung, R.E., Weers, D.C., Friedman, S.D., et al., 2000. Metabolic and cognitive response to human traumatic brain injury: a quantitative proton magnetic resonance study. J. Neurotrauma 17, 629–640.

Chauviere, L., Rafrafi, N., Thinus-Blanc, C., Bartolomei, F., Esclapez, M., Bernard, C., 2009. Early deficits in spatial memory and theta rhythmin experimental temporal lobe epilepsy. J. Neurosci. 29, 5402–5410.

Cilio, M.R., Sogawa, Y., Cha, B.H., Liu, X., Huang, L.T., Holmes, G.L., 2003. Long-term effects of status epilepticus in the immature brain are specific for age and model. Epilepsia 44, 518–528.

Coras, R., Siebzehnrubl, F.A., Pauli, E., Huttner, H.B., Njunting, M., Kobow, K., et al., 2010. Low proliferation and differentiation capacities of adult hippocampal stem cells correlate with memory dysfunction in humans. Brain 133, 3359–3372.

DeLorenzo, R.J., Pellock, J.M., Towne, A.R., Boggs, J.G., 1995. Epidemiology of status epilepticus. J. Clin. Neurophysiol. 12, 316–325.

Devinsky, O., Vezzani, A., Najjar, S., De Lanerolle, N.C., Rogawski, M.A., 2013. Glia and epilepsy: excitability and inflammation. Trends Neurosci. 36, 174–184.

Dubé, C., Boyet, S.,Marescaux, C., Nehlig, A., 2001. Relationship between neuronal loss and interictal glucose metabolism during the chronic phase of the lithium-pilocarpine model of epilepsy in the immature and adult rat. Exp. Neurol. 167, 227–241.

Duncan, J.S., Sander, J.W., Sisodiya, S.M., Walker, M.C., 2006. Adult epilepsy. Lancet 367, 1087–1100.

Elger, C.E., Helmstaedter, C., Kurthen, M., 2004. Chronic epilepsy and cognition. Lancet Neurol. 3, 663–672.

Engel Jr., J., Pitkanen, A., Loeb, J.A., Dudek, F.E., Bertram 3rd, E.H., Cole, A.J., et al., 2013. Epilepsy biomarkers. Epilepsia 54 (Suppl. 4), 61–69.

Filibian,M., Frasca, A., Maggioni, D., Micotti, E., Vezzani, A., Ravizza, T., 2012. In vivo imaging of glia activation using 1H-magnetic resonance spectroscopy to detect putative biomarkers of tissue epileptogenicity. Epilepsia 53, 1907–1916.

Frigerio, F., Frasca, A.,Weissberg, I., Parrella, S., Friedman, A., Vezzani, A., et al., 2012. Longlasting pro-ictogenic effects induced in vivo by rat brain exposure to serum albumin in the absence of concomitant pathology. Epilepsia 53, 1887–1897.
Fujikawa, D.G., 1996. The temporal evolution of neuronal damage from pilocarpineinduced status epilepticus. Brain Res. 725, 11–22.
Garnett, M.R., Blamire, A.M., Corkill, R.G., Cadoux-Hudson, T.A., Rajagopalan, B., Styles, P., 2000. Early proton magnetic resonance spectroscopy in normal-appearing brain correlates with outcome in patients following traumatic brain injury. Brain 123 (Pt 10), 2046–2054.
Gerlai, R.,Wojtowicz, J.M., Marks, A., Roder, J., 1995. Overexpression of a calcium-binding protein, S100 beta, in astrocytes alters synaptic plasticity and impairs spatial learning in transgenic mice. Learn. Mem. 2, 26–39.
Gray, W.P., Sundstrom, L.E., 1998. Kainic acid increases the proliferation of granule cell progenitors in the dentate gyrus of the adult rat. Brain Res. 790, 52–59.
Hattiangady, B., Rao,M.S., Shetty, A.K., 2004. Chronic temporal lobe epilepsy is associated with severely declined dentate neurogenesis in the adult hippocampus. Neurobiol. Dis. 17, 473–490.
Herman, S.T., 2002. Epilepsy after brain insult: targeting epileptogenesis. Neurology 59, S21–S26.
Hermann, B., Jones, J., Sheth, R., Dow, C., Koehn, M., Seidenberg, M., 2006. Children with new-onset epilepsy: neuropsychological status and brain structure. Brain 129, 2609–2619.
Hesdorffer, D.C., Logroscino, G., Cascino, G., Annegers, J.F., Hauser,W.A., 1998. Risk of unprovoked seizure after acute symptomatic seizure: effect of status epilepticus. Ann. Neurol. 44, 908–912.
Holmes, G.L., 2015. Cognitive impairment in epilepsy: the role of network abnormalities. Epileptic Disord 17, 101–116.
Holtkamp, M., Othman, J., Buchheim, K., Meierkord, H., 2005. Predictors and prognosis of refractory status epilepticus treated in a neurological intensive care unit. J. Neurol. Neurosurg. Psychiatry 76, 534–539.
Hort, J., Brozek, G., Komarek, V., Langmeier,M., Mares, P., 2000. Interstrain differences in cognitive
functions in rats in relation to status epilepticus. Behav. Brain Res. 112, 77–83.
Huttunen, H.J., Kuja-Panula, J., Sorci, G., Agneletti, A.L., Donato, R., Rauvala, H., 2000. Coregulation of neurite outgrowth and cell survival by amphoterin and S100 proteins through receptor for advanced glycation end products (RAGE) activation. J. Biol. Chem. 275, 40096–40105.
Iori, V., Maroso, M., Rizzi, M., Iyer, A.M., Vertemara, R., Carli, M., et al., 2013. Receptor for Advanced Glycation Endproducts is upregulated in temporal lobe epilepsy and contributes to experimental seizures. Neurobiol. Dis. 58, 102–114.
Jiang, M., Lee, C.L., Smith, K.L., Swann, J.W., 1998. Spine loss and other persistent alterations of hippocampal pyramidal cell dendrites in a model of early-onset epilepsy. J. Neurosci. 18, 8356–8368.
Jones, N.C., Martin, S., Megatia, I., Hakami, T., Salzberg, M.R., Pinault, D., et al., 2010. A genetic epilepsy rat model displays endophenotypes of psychosis. Neurobiol. Dis. 39, 116–125.
Kleen, J.K., Scott, R.C., Lenck-Santini, P.P., Holmes, G.L., 2012. Cognitive and behavioral comorbidities of epilepsy. In: Noebels, J.L., et al. (Eds.), Jasper's Basic Mechanisms of the

Epilepsies, fourth ed. National Center for Biotechnology Information (US), Bethesda (MD).
Kubova, H., Mares, P., Suchomelova, L., Brozek, G., Druga, R., Pitkanen, A., 2004. Status epilepticus in immature rats leads to behavioural and cognitive impairment and epileptogenesis. Eur. J. Neurosci. 19, 3255–3265.
Leroy, C., Pierre, K., Simpson, I.A., Pellerin, L., Vannucci, S.J., Nehlig, A., 2011. Temporal changes in mRNA expression of the brain nutrient transporters in the lithiumpilocarpine model of epilepsy in the immature and adult rat. Neurobiol. Dis. 43, 588–597.
Liu, Z., Gatt, A.,Werner, S.J.,Mikati,M.A., Holmes, G.L., 1994. Long-termbehavioral deficits following pilocarpine seizures in immature rats. Epilepsy Res. 19, 191–204.
Logroscino, G., Hesdorffer, D.C., Cascino, G., Annegers, J.F., Hauser,W.A., 1997. Short-term mortality after a first episode of status epilepticus. Epilepsia 38, 1344–1349.
Marcon, J., Gagliardi, B., Balosso, S., Maroso, M., Noe, F., Morin, M., et al., 2009. Agedependent vascular changes induced by status epilepticus in rat forebrain: implications for epileptogenesis. Neurobiol Dis 34, 121–132.
Mazarati, A., Maroso, M., Iori, V., Vezzani, A., Carli, M., 2011. High-mobility group box-1 impairs memory in mice through both toll-like receptor 4 and receptor for advanced glycation end products. Exp. Neurol. 232, 143–148.
Morquette, P., Verdier, D., Kadala, A., Fethiere, J., Philippe, A.G., Robitaille, R., et al., 2015. An astrocyte-dependent mechanism for neuronal rhythmogenesis. Nat. Neurosci. 18, 844–854.
Nishiyama, H., Knopfel, T., Endo, S., Itohara, S., 2002. Glial protein S100B modulates longterm neuronal synaptic plasticity. Proc. Natl. Acad. Sci. U. S. A. 99, 4037–4042.
Oostrom, K.J., Smeets-Schouten, A., Kruitwagen, C.L., Peters, A.C., Jennekens-Schinkel, A., 2003. Not only amatter of epilepsy: early problems of cognition and behavior in children with “epilepsy only”–a prospective, longitudinal, controlled study starting at diagnosis. Pediatrics 112, 1338–1344.
Parent, J.M., Yu, T.W., Leibowitz, R.T., Geschwind, D.H., Sloviter, R.S., Lowenstein, D.H., 1997. Dentate granule cell neurogenesis is increased by seizures and contributes to aberrant network reorganization in the adult rat hippocampus. J. Neurosci. 17, 3727–3738.
Paxinos, G., Watson, C., 2005. The Rat Brain in Stereotaxic Coordinates. Academic Press, New York.
Pitkanen, A, Engel, Jr., J, Past and present definitions of epileptogenesis and its biomarkers. Neurotherapeutics 2014;11:231–41. Pitkanen, A., Kharatishvili, I., Narkilahti, S., Lukasiuk, K., Nissinen, J., 2005. Administration of diazepam during status epilepticus reduces development and severity of epilepsy in rat. Epilepsy Res. 63, 27–42.
Raspall-Chaure,M., Chin, R.F., Neville, B.G., Scott, R.C., 2006. Outcome of paediatric convulsive status epilepticus: a systematic review. Lancet Neurol. 5, 769–779.
Robel, S., Buckingham, S.C., Boni, J.L., Campbell, S.L., Danbolt, N.C., Riedemann, T., et al., 2015. Reactive astrogliosis causes the development of spontaneous seizures. J. Neurosci. 35, 3330–3345.
Roch, C., Leroy, C., Nehlig, A., Namer, I.J., 2002. Predictive value of cortical injury for the development of temporal lobe epilepsy in 21-day-old rats: an MRI approach using the lithium-pilocarpine model. Epilepsia 43, 1129–1136.
Sakatani, S., Seto-Ohshima, A., Shinohara, Y., Yamamoto, Y., Yamamoto, H., Itohara, S., et al., 2008. Neural-activity-dependent release of S100B from astrocytes enhances kainate-induced gamma oscillations in vivo. J. Neurosci. 28, 10928–10936.

Sayin, U., Sutula, T.P., Stafstrom, C.E., 2004. Seizures in the developing brain cause adverse long-term effects on spatial learning and anxiety. Epilepsia 45, 1539–1548.
Scharfman, H.E., Gray, W.P., 2007. Relevance of seizure-induced neurogenesis in animal models of epilepsy to the etiology of temporal lobe epilepsy. Epilepsia 48 (Suppl. 2), 33–41.
Scharfman, H.E., Goodman, J.H., Sollas, A.L., 2000. Granule-like neurons at the hilar/CA3 border after status epilepticus and their synchrony with area CA3 pyramidal cells: functional implications of seizure-induced neurogenesis. J. Neurosci. 20, 6144–6158.
Spigolon, G., Veronesi, C., Bonny, C., Vercelli, A., 2010. c-Jun N-terminal kinase signaling pathway in excitotoxic cell death following kainic acid-induced status epilepticus. Eur. J. Neurosci. 31, 1261–1272.
Todd, K.J., Serrano, A., Lacaille, J.C., Robitaille, R., 2006. Glial cells in synaptic plasticity. J. Physiol. Paris 99, 75–83.
Vezzani, A., Auvin, S., Ravizza, T., Aronica, E., 2012. Glia-neuronal interactions in ictogenesis and epileptogenesis: role of inflammatory mediators. In: Noebels, J.L., et al. (Eds.), Jasper's Basic Mechanisms of the Epilepsies, fourth ed. National Center for Biotechnology Information (US), Bethesda (MD).
Vezzani, A., French, J., Bartfai, T., Baram, T.Z., 2011. The role of inflammation in epilepsy. Nat Rev Neurol 7, 31–40.
Wagenman, K.L., Blake, T.P., Sanchez, S.M., Schultheis, M.T., Radcliffe, J., Berg, R.A., et al., 2014. Electrographic status epilepticus and long-term outcome in critically ill children. Neurology 82, 396–404.
Wilson, M., Reynolds, G., Kauppinen, R.A., Arvanitis, T.N., Peet, A.C., 2011. A constrained least-squares approach to the automated quantitation of in vivo (1)H magnetic resonance spectroscopy data. Magn. Reson. Med. 65, 1–12.
Witt, J.A., Helmstaedter, C., 2015. Cognition in the early stages of adult epilepsy. Seizure 26, 65–68.
Wu, Y., Pearce, P.S., Rapuano, A., Hitchens, T.K., de Lanerolle, N.C., Pan, J.W., 2015. Metabolic changes in early poststatus epilepticus measured by MR spectroscopy in rats. J. Cereb. Blood Flow Metab. 35, 1862–1870.
Zaben, M., Sheward,W.J., Shtaya, A., Abbosh, C., Harmar, A.J., Pringle, A.K., et al., 2009. The neurotransmitter VIP expands the pool of symmetrically dividing postnatal dentate gyrus precursors via VPAC2 receptors or directs them toward a neuronal fate via VPAC1 receptors. Stem Cells 27, 2539–2551.
Zahr, N.M., Crawford, E.L., Hsu, O., Vinco, S.,Mayer, D., Rohlfing, T., et al., 2009. In vivo glutamate decline associated with kainic acid-induced status epilepticus. Brain Res. 1300, 65–78